Published in final edited form as:
Anat Rec (Hoboken). 2009 August ; 292(8): 1162–1181. doi:10.1002/ar.20935.

The Mesencephalic Reticular Formation as a Conduit for Primate Collicular Gaze Control: Tectal Inputs to Neurons Targeting the Spinal Cord and Medulla

Eddie Perkins[1,4], **Susan Warren**[1], and **Paul J. May**[1,2,3]

[1]Department of Anatomy, University of Mississippi Medical Center, 2500 North State Street, Jackson, MS 39216-4505 U.S.A.

[2]Department of Ophthalmology, University of Mississippi Medical Center, 2500 North State Street, Jackson, MS 39216-4505 U.S.A.

[3]Department of Neurology, University of Mississippi Medical Center, 2500 North State Street, Jackson, MS 39216-4505 U.S.A.

[4]Department of Neurosurgery, University of Mississippi Medical Center, 2500 North State Street, Jackson, MS 39216-4505 U.S.A.

Abstract

The superior colliculus (SC), which directs orienting movements of both the eyes and head, is reciprocally connected to the mesencephalic reticular formation (MRF), suggesting the latter is involved in gaze control. The MRF has been provisionally subdivided to include a rostral portion, which subserves vertical gaze, and a caudal portion, which subserves horizontal gaze. Both regions contain cells projecting downstream that may provide a conduit for tectal signals targeting the gaze control centers which direct head movements. We determined the distribution of cells targeting the cervical spinal cord and rostral medullary reticular formation (MdRF), and investigated whether these MRF neurons receive input from the SC by the use of dual tracer techniques in *Macaca fascicularis* monkeys. Either biotinylated dextran amine or *Phaseolus vulgaris* leucoagglutinin was injected into the SC. Wheat germ agglutinin conjugated horseradish peroxidase was placed into the ipsilateral cervical spinal cord or medial MdRF to retrogradely label MRF neurons. A small number of medially located cells in the rostral and caudal MRF were labeled following spinal cord injections, and greater numbers were labeled in the same region following MdRF injections. In both cases, anterogradely labeled tectoreticular terminals were observed in close association with retrogradely labeled neurons. These close associations between tectoreticular terminals and neurons with descending projections suggest the presence of a trans-MRF pathway that provides a conduit for tectal control over head orienting movements. The medial location of these reticulospinal and reticuloreticular neurons suggests this MRF region may be specialized for head movement control.

Keywords

head movement; oculomotor; superior colliculus; reticular formation; gaze

Corresponding Author: Paul J May, PhD, Department of Anatomy, University of Mississippi Medical Center, 2500 North State Street, Jackson, MS 39216-44505, pmay@anatomy.umsmed.edu, Phone: 610/984-1662, Fax: 601/984-1655.

INTRODUCTION

Animals explore their environment using a series of gaze changes in which quick accompanying head movements are often employed in conjunction with saccades to help bring selected targets onto the fovea, and to reset the eyes near primary position. While we have considerable knowledge of the circuitry that controls eye movements during gaze changes, our understanding of the circuits controlling the head components is less complete (Guitton et al., 1984; André-Deshays et al., 1991; Fuller, 1992; Tweed et al., 1995; Stahl, 1999; Freedman and Sparks, 2000). The superior colliculus (SC) is the primary brainstem center for computing the vector of a gaze change (Sparks, 1986). By use of preparations in which the head is unrestrained, it has been shown that SC gaze signals direct movements of the head, as well as the eyes (Stryker and Schiller, 1975; Roucoux et al., 1980; Cowie and Robinson, 1994; Freedman and Sparks, 1997a&b; Walton et al., 2007). The main gaze-related outflow of the SC via the predorsal bundle or crossed tectobulbospinal pathway reaches the upper cervical cord (Anderson et al., 1971; Harting, 1977; Nudo and Masterton, 1989; May and Porter, 1992; Cowie et al., 1994; Robinson et al., 1994). However, the projections to the spinal cord are relatively sparse in monkeys, and only a limited number of terminals in the spinal cord directly contact motoneurons (Rose et al., 1991; May and Porter, 1992). Instead, the main control of gaze-related head movements appears to lie within the rostromedial medullary reticular formation (MdRF). Electrical stimulation of the paramedian portion of the gigantocellular medullary reticular formation between the levels of the abducens and hypoglossal nuclei produces head movements like those seen with gaze changes (Iwamoto et al., 1988; Drew and Rossignol, 1990a&b; Cowie et al., 1994; Cowie and Robinson, 1994; Quessy and Freedman, 2004). This region contains reticulospinal neurons that receive collicular inputs and fire before head movements in conjunction with gaze changes (Isa and Nito, 1995; Kakei et al., 1994).

While the collicular pathways projecting directly and indirectly to the upper cervical spinal cord would appear to provide a necessary substrate for tectally-initiated head movements, it should be recalled that interactions between the head and eye are complex, and can be modified by the context of a gaze change (Ron and Berthoz, 1991; Fuller, 1992; Dunham, 1997; Stahl, 2001; Sylvestre and Cullen, 2006). Moreover, the steps required to transform the spatial code for gaze movement present in the SC into the temporal code by which motoneurons direct the musculature have yet to be fully specified (Moschovakis et al., 1998; Badler and Keller, 2002). Even at the level of the neck musculature, the activity of the various muscles appears to be regulated in a complex manner, due to the numerous joints involved and the head's large mass compared to the eye (Richmond et al., 1992; Thomson et al., 1996; Corneil et al., 2001). In light of these facts, it is reasonable to investigate whether other structures play a role in tectal control over head movements.

Among structures receiving collicular input, the mesencephalic reticular formation (MRF) is particularly well endowed with tectal terminals (Harting, 1977; Huerta and Harting, 1982; Chen and May, 2000). The MRF has been subdivided into a rostral portion adjacent to (peri) the interstitial nucleus of Cajal (piMRF), which is believed to be involved in the vertical component of gaze changes, and a caudal portion, the central mesencephalic reticular formation (cMRF), which is believed to be involved in horizontal gaze changes (King et al., 1980; Cohen et al., 1985; Scudder et al., 1996a; Waitzman et al., 1996; Waitzman et al., 2000a&b). Many of the neurons within the MRF show firing characteristics that are similar to those of collicular or paramedian pontine reticular formation (PPRF) neurons (King et al., 1980; Moschovakis et al., 1988b; Fukushima et al., 1995; Scudder et al., 1996a&b; Cromer and Waitzman, 2007). This may not be surprising as collaterals of the predorsal bundle axons terminate extensively in the ipsilateral MRF (Grantyn and Grantyn, 1982; Moschovakis and Karabelas, 1985; Moschovakis et al., 1988a). Lesions in or chemical

inactivation of the MRF impairs the accuracy of gaze changes and modifies head position (Bender and Shanzer, 1964; Waitzman et al., 2000a&b). Furthermore, cMRF recordings made in head-free monkeys indicate that while most cell activity correlates with gaze, some neurons have activity that correlates best with head movements (Pathmanathan et al., 2006a&b). However, the manner in which the cMRF and/or piMRF fit into the anatomical circuits for control of eye and head movements is not well understood. The purpose of the present study was to investigate this point. Specifically, a dual tracer approach was used in macaque monkeys to determine the relationship between tectoreticular axonal arbors and MRF neurons that project to the cervical spinal cord or MdRF. Portions of this work have been described previously in abstract form (May et al., 2005).

MATERIALS AND METHODS

This study was carried out in 8 juvenile or young adult macaque monkeys (*Macaca fascicularis*). All of the experiments were performed in accordance with NIH guidelines for animal care and use, using protocols approved by the local IACUC.

Surgical Procedure

The injection paradigm required sequential surgical procedures with an interval based on the transport times of the tracers. The collicular, brainstem and spinal cord injections were all placed on the left side. The anterograde tracers BDA (biotinylated dextran amine, N=6) or PhaL (*Phaseolus vulgaris* leukoagglutinin, N=2), were injected into the SC. Approximately 3 weeks after the BDA injections, WGA-HRP (wheat germ agglutinin-horseradish peroxidase) was placed into the spinal cord of 2 animals, or the MdRF of 4 animals. Approximately 2 weeks after the PhaL injections, WGA-HRP was placed in the MdRF of 2 animals. Animals were sacrificed within 48 hours of the second tracer injection.

Before surgery, monkeys were sedated with ketamine HCL (10 mg/kg, IM). A surgical level of anesthesia was induced and maintained with isoflurane (2–3%). Dexamethasone (0.4 mg, IV) was given to minimize cerebral edema, and atropine sulfate (0.05 mg/kg, IM) was given to reduce airway secretions. The left SC was visualized via a unilateral craniotomy, followed by aspiration of the medial bank of parietal and occipital cortex where it overlies the SC and rostral vermis. A solution of 10 % BDA was pressure injected using a 1.0 μl Hamilton syringe angled 20° tip rostral in the sagittal plane. Two injections of 0.1–0.2 μl each were placed between 1.0–1.5 mm beneath the collicular surface. Alternatively, a solution of 2.5 % PhaL in 0.1 M, pH 8.0 phosphate buffer, which was contained in a glass micropipette (20–30 μm tip), was iontophoresed into the SC by passing a positive current of 5–10 μA for 10 minutes (50% duty cycle, 7 sec/pulse). The defect left by the aspiration was filled with gelfoam and the wound edges were re-apposed and sutured. The wound site was treated with a local anesthetic (Sensorcaine, SC). Post-operatively, the animals were treated with the analgesic, Buprenex (0.01 mg/kg, IM).

Each animal underwent a second surgery to inject the spinal cord or MdRF. A 1–2 % solution of WGA-HRP mixed with a 10% solution of horseradish peroxidase (HRP) was pressure injected using a 1.0 μl Hamilton syringe. The general procedures for the second surgery were the same as those used for the first surgery, but a posterior approach was taken. After being positioned in the stereotaxic headholder, the animal's head was angled to 33°, nose down. The skin and muscle between the nuchal crest and C1 were incised along the midline and retracted laterally. The atlanto-occipital membrane was incised. For the spinal cord injections, a portion of the C1 vertebral arch was removed. The needle was then advanced to a depth of 2–3 mm below the surface with the syringe angled to pierce the surface of the cord orthogonally, through the dorsal columns. Injections of 0.1μl each were made at 2–3 different rostrocaudal sites. For the medullary injections, the microsyringe was

instead directed at an angle of 67–80°, tip rostral in the sagittal plane, to penetrate to the MdRF by entering through the dorsal medullary surface. Stereotaxic coordinates for the MdRF (8.0 posterior, 2.0 lateral, 1.0 dorsal) (Szabo and Cowan, 1984) were adjusted with respect to the coordinates of the obex. Injection ranging from 0.02 to 0.05 µl were made at 1–3 points along the track. Following either type of injection, the cisterna magna was sealed by placing Gelfilm beneath the atlanto-occipital membrane. The muscle layers and skin were re-apposed and stabilized with suture. As before, local and general analgesics were administered during the postoperative period. Animals were sacrificed 24–48 hours after the WGA-HRP injection in all cases. Each monkey received an overdose of sodium pentobarbital (50 mg/kg, IP), and was perfused transcardially. A buffered saline prewash, was followed by a fixative solution of 1.0 % paraformaldehyde and 1.25–1.5 % glutaraldehyde in 0.1 M, pH 7.2 phosphate buffer (PB). Brains were blocked in the frontal plane, post fixed 1–2 hours in the same fixative, and then stored over night at 4° C in PB.

Histological Procedures

Brainstem sections were cut in the frontal plane and spinal cord sections were cut longitudinally at 100 µm by use of a vibratome (Leica). Two sets of 1 in 3 series, in which the sections were 300 µm apart, were processed sequentially to reveal both the WGA-HRP and the BDA or PhaL reaction product (Chen and May, 2002). First, the tissue was reacted to demonstrate the WGA-HRP by use of a tetramethylbezidine (TMB) protocol. Briefly, the sections were rinsed with 0.1 M, pH 6.0 PB, followed by preincubation in 0.005 % TMB (tetramethylbenzidine HCl), 0.25 % ethanol, and 0.245 % ammonium molybdate in 0.1M, pH 6.0 PB. The reaction was initiated by the addition of H_20_2 solution (0.011 %), and the sections incubated overnight at 4°C. They were then transferred to a stabilizer solution of 5.0 % ammonium molybdate in 0.1 M, pH 6.0 PB, followed by multiple rinses in the same PB. These sections were further stabilized by incubation in a 5.0 % solution of DAB (diaminobenzidine HCl) in 0.1 M, pH 7.2 PB to which H_2O_2 (0.011 %) was added to produce a brown reaction product in the labeled neurons.

To demonstrate the transported tracer in animals with BDA injections, the tissue was rinsed in 0.1 M, pH 7.2 PB after the TMB and DAB procedures. It was then introduced to 0.5 % triton X-100 in 0.1 M, pH 7.2 PB. Next, sections were incubated overnight at 4°C in an Avidin-HRP (Vector Laboratories) solution (1:500) in 0.1 M, pH 7.2 PB containing 0.05 % triton X-100. After rinsing with 0.1 M, pH 7.2 PB, they were reacted in a 5.0 % DAB solution of 0.1M, pH 7.2 PB containing 0.011 % H_2O_2, 0.05 % nickel ammonium sulfate and 0.025–0.05 % cobalt chloride for 10–30 minutes to produce a black reaction product in labeled axons.

To demonstrate the transported tracer in animals with PhaL injections, the sections were rinsed in 0.1M, pH 7.2 PB after the TMB and DAB procedures. Next, sections were incubated in 0.3% triton X-100, 10 % normal goat serum (NGS) solution in 0.1 M, pH 7.2 PB. These sections were then incubated with goat biotinylated anti-PhaL (1:200 in 0.1M, pH 7.2 PB solution) with 10 % NGS overnight at 4°C. Next, the sections were incubated with the final ABC Kit solution (Vector Laboratories) for 1–2 hours. Sections were rinsed in 0.1M, pH 7.2 PB, then they were incubated in a 5.0 % DAB, 0.05 % nickel ammonium sulfate solution with 0.011 % H_2O_2 in 0.1M, pH 7.2 PB. Additional 1 in 6 series were reacted to demonstrate the presence and distribution of the WGA-HRP (TMB) or BDA (Avidin-HRP-DAB) or PhaL (biotinylated anti-PhaL, ABC, nickel/cobalt DAB) alone, by use of the appropriate parts of the techniques described above. In all cases, the sections were rinsed in 0.1M, pH 7.2 PB, mounted on gelatinized slides, counterstained in cresyl violet, dehydrated, cleared and coverslipped .

Data Analysis

The distributions of anterogradely labeled tectoreticular axon terminals and retrogradely labeled neurons were charted at 32× magnification, and individual neurons and axons exhibiting close associations were drawn at 800× magnification using an Olympus BH-2 or Nikon Eclipse 80i microscope equipped with a drawing tube. Selected areas within the MRF that contained labeled neurons and terminals were digitally photographed with a Nikon Eclipse E600 photomicroscope equipped with Nikon Digital DXM1200F camera by use of MetaMorph image analysis software. Digitized information from up to 20 Z-axis focal planes 1 μm apart was combined into a single plane by use of the MetaMorph "stack arithmetic minimum" function. The brightness, contrast and color of the digitized images were adjusted in Adobe Photoshop to appear as close as possible to the visualized image.

RESULTS

The brainstem region identified as the cMRF occupies roughly the central half of the MRF's dorsoventral dimension. It extends from just rostral of the level of the nucleus of the posterior commissure to the level of the trochlear nucleus. The piMRF is located immediately rostral to this, at the levels where the interstitial nucleus of Cajal (InC) is present. These definitions are based on physiological studies (Cohen et al., 1985; Waitzman et al., 1996, 2000 a&b), and examination of the MRF following injections of tracer into the SC (Chen and May, 2000; Warren et al., 2008).

Tectoreticulospinal Connections

Injections of the bidirectional tracer, BDA, into the SC labeled both reticulotectal cells and tectoreticular axons in MRF. The WGA-HRP was used to retrogradely label reticulospinal neurons in MRF. The 2 animals with these injections showed similar MRF labeling patterns. One case is shown in figure 1. The collicular injection included all layers of the caudal SC and extended into the intercollicular zone ventral to SC (insert upper right). Based on measurements made of roots upon extracting the spinal cord, the WGA-HRP injection in this case extended from C1 to C2 (insert lower right). It included both the dorsal and ventral horns, and adjacent areas of white matter on the left, but also extended across the midline to include the gray matter on the right side.

As a result of the SC injection, a region was present in the left caudal MRF that contained extensive overlap between BDA labeled tectoreticular axon terminals (stipple) and BDA labeled reticulotectal cells (dots) (Fig. 1B–D). We have proposed that the region of overlap between the BDA labeled terminals and BDA labeled neurons represents the cMRF (Chen and May, 2000).

While labeled tectoreticular terminals were observed rostrally in the piMRF, labeled reticulotectal cells were not (Fig. 1A). BDA labeled reticulotectal neurons were also found in the cMRF contralateral to the SC injection, but there were few BDA labeled tectoreticular terminals on this side. The neurons labeled with WGA-HRP following the cervical cord injection (diamonds, Fig. 1) lay within the gaze-related portion of the midbrain, as defined by the anterogradely labeled terminal field from the SC injection. Most reticulospinal neurons were located medially, adjacent to the central gray, in both the piMRF (Fig. 1A) and cMRF (Fig. 1B–D). Fewer retrogradely labeled cells were observed in the material reacted to show both tracers compared to sections reacted to reveal just the WGA-HRP (see Warren et al., 2008) suggesting some loss of lightly labeled cells in the dual tracer procedure.

The relationship between the BDA labeled tectoreticular axonal arbors and the WGA-HRP labeled reticulospinal cells in the MRF is illustrated in figure 2. Reticulospinal neurons in both the piMRF (Fig. 2A&B) and cMRF (Fig. 2C–F) were medium sized, multipolar cells.

They lay within a field of poorly branched, BDA labeled, tectoreticular terminal arbors, that displayed *en passant* and terminal boutons. In some cases, BDA labeled boutons lay in close association (arrowheads) with the retrogradely labeled reticulospinal neurons within the piMRF (Fig. 2A&B) and cMRF (Fig. 2F).

The difference between the BDA and WGA-HRP labeling is shown in figure 3A. The BDA labeled reticulotectal neurons (red arrow) were darker in color than the golden brown color of the labeled reticulospinal neurons (blue arrow). Close associations (arrowheads) can be seen between the BDA labeled tectoreticular axonal boutons and the somata (Fig. 3A&C) and dendrites (Fig. 3B) of these reticulospinal neurons, in the piMRF (Fig. 3C) and cMRF (Fig. 3A&B).

MRF reticuloreticular neurons

Cases in which the tissue was reacted using just the TMB protocol were plotted to determine the distribution of the WGA-HRP labeled reticuloreticular neurons in the MRF that project to the medulla. Figure 4 shows the pattern of retrograde label from an injection site that was located primarily in left MdRF with some extension over the midline, and limited spread into the inferior olive (Fig. 4G–I). Rostrally (Fig. 4A&B), retrogradely labeled neurons (dots) were located ipsilaterally in the piMRF, as well as in the interstitial nucleus of Cajal (InC) and nucleus of Darkschiewitsch (nD). Labeled piMRF cells were mainly found medially, adjacent to the InC. Caudally (Fig. 4C–E), retrogradely labeled cells were observed in the medial half of the cMRF. A few labeled cells were also present in adjacent regions of the periaqueductal gray. The labeled neurons located in the nucleus of the optic tract (Fig. 4E&F) are presumably due to inclusion of the inferior olive in the injection site (Mustari et al., 1994).

Tectoreticuloreticular Connections

BDA Experiments—In order to determine whether the SC utilizes the MRF to control head movement areas within the medulla, injections of BDA and WGA-HRP were placed into the SC and MdRF, respectively. Similar patterns of label were observed in the 4 cases. In the illustrated example, BDA placed into the left SC involved portions of all the collicular layers (Fig. 5A–D & 6A), and minimally invaded the dorsolateral portion of the periaqueductal gray (Fig. 5A&B). The tracer was confined to the middle third of the SC, in its mediolateral dimension. The injection of WGA-HRP in the same animal was directed into the medial MdRF on the same side (Fig. 5D–G & 6B). The injection site was centered off the midline with minimal spread into the opposite side (Fig. 5D). The core of the injection was found in the paramedian medullary reticular formation, caudal to the level of the abducens nucleus. Due to the angled approach, the track entered the surface of the open medulla caudally, at the level of the hypoglossal nucleus and ended rostrally within the inferior olive at the level of the abducens nucleus (Fig. 5D). However, the tracer did not encroach upon the PPRF.

As in the collicular injection described earlier, labeled tectoreticular terminals, as well as reticulotectal neurons, were seen within the MRF ipsilateral to the SC injection (Fig. 7). Caudally, BDA labeled tectoreticular terminals (stipple) were again widely distributed within the cMRF (Fig. 7C–G), and extended rostrally into the piMRF (Fig. 7A&B). BDA labeled reticulotectal neurons (black dots) were again concentrated as a mediolaterally oriented band extending across the cMRF (Fig. 7C–G), but were largely absent from the piMRF (Fig. 7A&B). Reticuloreticular neurons labeled retrogradely from the WGA-HRP injection in the MdRF (diamonds) were also found within the piMRF (Fig. 7A&B) and cMRF (Fig. 7C–G). Again, fewer retrogradely labeled cells were observed in the dual tracer material (Fig. 7) in comparison to sections reacted just for WGA-HRP (Fig. 4). Most of the

WGA-HRP labeled reticuloreticular neurons in the cMRF were located in its medial half (Fig. 7C–G). In the piMRF the vast majority of WGA-HRP labeled neurons were also observed medially within the MRF, and appeared to be continuous with labeled neurons within the adjacent nucleus of Darkschewitsch (nD) (Fig. 7A&B). More labeled neurons were located dorsally and dorsolaterally in the MRF of this case than the others, and fewer were present in InC (Fig. 4), perhaps due to greater spread of the tracer. WGA-HRP labeled neurons were also seen in the periaqueductal gray (Fig. 7A–G), and the supraoculomotor area (Fig. 7C–E).

The overlap in the distribution of the retrogradely labeled reticuloreticular neurons and the anterogradely labeled tectoreticular terminals in the MRF suggested the possibility of connections between the two elements. Figure 8 provides illustrations of these possible connections. The labeled reticuloreticular neurons in the piMRF (Fig. 8A) and cMRF (Fig. 8B) were multipolar, with 3–4 primary dendrites. Their somata ranged in size from 40–60 μm along their long axis. The labeled tectoreticular terminal arbors rarely displayed branches, and appeared as thin segments connecting *en passant* boutons of slightly different sizes. Specifically, in the piMRF (Fig. 8A), close associations (arrowheads) between labeled axonal boutons, and the somata (Fig. 8A, cells a,b,c&f) and dendrites (Fig. 8A, cells a–f) of the labeled cells were apparent. Very similar relationships were observed between WGA-HRP labeled reticuloreticular neurons and BDA labeled tectoreticular axons more caudally, in the cMRF (Fig. 8B). Close associations (arrowheads) were observed between these boutons and the somata (Fig. 8B, cells b,c,e,f&g) and dendrites (Fig. 8B, cells a,b,d–g) of the retrogradely labeled reticuloreticular neurons. In both the cMRF and piMRF, an individual axon was generally seen to make only a few contacts with any individual reticuloreticular cell, although individual cells often received several contacts from different axons (e.g., Fig. 8A, cells a&b; 8B, cell b).

Figure 3D shows the two populations of neurons that were retrogradely labeled following tectal and MdRF injections. In general, the black reticulotectal cells appeared to be larger than the brown reticuloreticular neurons, but this impression may be due to the better dendritic filling provided by the BDA. Close associations (arrowheads) between the BDA labeled (black) tectoreticular axon terminals and WGA-HRP labeled (brown) reticuloreticular neurons were present in both the piMRF (Fig. 3E) and cMRF (Fig. 3F&G). In some cases, an individual axon displayed several boutonal close associations with the same cell (Fig. 3E&G). Labeled boutons were found in association with both the somata (Fig. 3E–G) and dendrites (Fig. 3 F&G) of these retrogradely labeled neurons.

PhaL Experiments—BDA is an effective anterograde tracer, but as shown above, it can also transport retrogradely. This presented a potential problem, as it was possible that labeling of reticulotectal axon collaterals within the cMRF could lead to confusion with anterogradely labeled tectoreticular terminals. In order to control for this, *Phaseolus vulgaris* leucoagglutinin (PhaL) injections of the SC were also employed. Figure 9 shows the location of the PhaL injection placed into the left SC, and WGA-HRP injection within the left MdRF of a representative example. The PhaL injections were centered in the intermediate gray layer of the caudal SC (Fig. 9A–C) with some extension into the deep gray layer. They spared the more medial and lateral regions of the SC. After entering the open medulla rostral to the hypoglossal nucleus, the WGA-HRP injection extended within the MdRF just lateral of the midline, to end medial to the inferior olive (Fig. 9C–F). There was little spread across the midline and the PPRF was not involved.

The pattern of terminal label (stipple) following this PhaL injection into the SC is shown in figure 10. Terminals were found throughout the rostrocaudal extent of MRF, including both the piMRF (Fig. 10A&B) and cMRF (Fig. 10C–G). The labeled tectoreticular terminals

were sparser than observed following the BDA injections (Fig. 4). No neurons labeled retrogradely with PhaL were present. The reticuloreticular neurons labeled retrogradely from the MdRF injection of WGA-HRP (dots) fell within this terminal field. As before, they were primarily located in the medial portion of the cMRF (Fig. 10C–G) and in the piMRF adjacent to labeled cells in the InC and nD (Fig. 10A&B).

The PhaL injections produced labeled axons that could be followed for considerable distances within the piMRF (Fig. 11A, cell c) and the cMRF (Fig. 11B, cell e). These axons branched occasionally, often displaying short side branches. They had both *en passant* and terminal boutons that varied slightly in size. Some of these labeled boutons were observed in close association with retrogradely labeled reticuloreticular neurons in the piMRF (Fig. 11A) and cMRF (Fig. 11B). Close associations (arrowheads) between these tectoreticular boutons and the somata (Fig. 11A, cells b–e; 11B, cells a, c–e) and dendrites (Fig. 11A, cells a–e; 11B, cells a–e) of the retrogradely labeled reticuloreticular neurons were readily apparent. These associations were similar to those seen with paired BDA and WGA-HRP injections (Fig. 8). In most cases, individual axons only contributed a few boutons to any individual retrogradely labeled neuron (e.g., Fig. 11B, cell a). In other cases, more extensive relationships were apparent (Fig. 11A, cells a–c; Fig 11B, lower cell d).

The photomicrographs in figure 12 further document the relationship between tectoreticular terminals and reticuloreticular neurons. These plates show examples of the close association (arrowheads) between WGA-HRP labeled reticuloreticular neurons and PhaL labeled tectoreticular terminals in the piMRF (Fig. 12A&B) and cMRF (Fig. 12C–F). In some cases (Fig. 12A,C&F), an individual PhaL labeled axon ran along the soma or dendrites of a labeled neuron providing numerous close associations between boutons and the cell. More commonly, an individual axon only provided a few associations with any particular neuron (Fig. 12B&C).

DISCUSSION

This study indicates that the distribution of tectoreticular terminals within the midbrain reticular formation overlaps that of reticulospinal neurons projecting to the upper cervical spinal cord, as well as reticuloreticular neurons projecting to the medullary reticular formation. Both of these populations of output neurons are largely confined to the medial half of the MRF, providing strong anatomical evidence that the medial MRF is in a position to influence gaze associated head movements. While previous studies have examined the distribution of these MRF populations, this is the first to allow simultaneous examination of the terminal and cell populations in a primate. Furthermore, the boutons of tectoreticular axons often displayed close associations with MRF neurons projecting to the MdRF and spinal cord, suggesting a synaptic connection. This indicates the presence of a mostly ipsilaterally directed, trans-MRF pathway for tectal control of head movements that runs in parallel with the decussating, direct collicular projections for head control.

In tracer studies, spread outside the target or labeling of axons-of-passage must be considered. Our cases included examples where the tracer did not spread beyond the confines of the SC, and the organization of the SC minimizes fiber-of-passage problems. In addition, we confirmed our BDA results with PhaL injections. WGA-HRP injections into the spinal cord present a fiber-of-passage problem, as we can not guarantee that the MRF neurons labeled in the present study did not actually project to more caudal segments. However, there is evidence that the MRF does not project far beyond the upper cervical cord (Fukushima et al., 1979; Zhou et al., 2006). Placement of tracer into the MdRF did produce considerable spread of tracer along the needle track, variously including the inferior olive, nucleus prepositus, and hypoglossal and gracile nuclei. Since the pattern of retrograde MRF

label did not change appreciably, despite variations in tracer spread into these nuclei, we believe this labeling of cells was not due to the inclusion of these structures. This opinion is supported by evidence that cMRF projections are confined to the paramedian MdRF (Zhou et al., 2006). Finally, it should be noted that while the close associations we observed certainly suggest synaptic contact, this remains to be confirmed by ultrastructural analysis. On the other hand, the close associations observed in the present study may represent only a fraction of the tectal input to these cMRF populations, as it was not possible to see terminal/cell associations out on the dendritic tree where the retrograde tracer failed to penetrate.

It is likely that the MRF and MdRF have multiple functions, but the pattern of connections, as summarized in Figure 13 suggests this part of the circuitry subserves gaze (Harting, 1977; Moschovakis et al., 1988b; Chen and May, 2000; Warren et al., 2008; Zhou et al., 2008). Neurons in the SC provide collicular input to the *ipsilateral* piMRF and cMRF. These same fibers constitute the crossed predorsal bundle pathway, which supplies input to the MdRF and cervical cord, in order to initiate head movements in combination with saccades. We have identified three populations of MRF neurons that are targeted by SC input: 1. reticulotectal cells that provide feedback to the superior colliculus (Chen and May, 2000; Warren et al., 2008); 2. reticuloreticular neurons that supply input to the ipsilateral medullary reticular formation head control zone (present results); and 3. reticulospinal neurons that project directly to the upper segments of the ipsilateral spinal cord (present results; Warren et al., 2008). The latter two are found medially within the MRF, while the first is found throughout the MRF. These results suggest that in addition to the crossed tectobulbospinal pathway emanating from the SC, an alternate circuit involving neurons in the ipsilateral MRF exists, which could provide a route whereby the colliculus influences head movements that occur with gaze changes. This trans-MRF pathway supplies the same target structures on the ipsilateral side as are supplied by the predorsal bundle pathway on the contralateral side.

Comparison to Previous Findings

In this study, we have concentrated on two MRF subdivisions: the rostral piMRF and caudal cMRF, to ease comparison with contemporary physiological studies of the region (Waitzman et al., 2000a&b; Cromer and Waitzman, 2006; Pathmanathan et al., 2006a&b). These studies and others (King et al., 1980; Scudder et al., 1996a) suggest that piMRF is more involved with vertical eye movement components, while the cMRF is more involved with horizontal eye movement components. However, neither the degree to which these are truly separate functions (Handel and Glimcher, 1997), nor the precise border between the subdivisions, have been defined. Our studies have highlighted a further difference, the fact that the ipsilateral piMRF largely lacked retrogradely labeled reticulotectal neurons following caudal SC injections (Chen and May, 2000; May, 2006; Warren et al., 2008). However, in a study in cats, we found reticulotectal neurons in the piMRF when more rostral regions of the SC contained tracer (May et al., 2002). So the piMRF may project preferentially to collicular regions containing the vertical meridian representation, while the cMRF projects more caudally.

A number of studies have shown a projection from the intermediate layer of the SC to the MRF (Harting, 1977; Huerta and Harting, 1982; Cohen and Büttner-Ennever, 1984; Chen and May, 2000; Zhou et al., 2008). Based on intra-axonal staining, there is good evidence that predorsal bundle axons carrying gaze-related activity provide collaterals that terminate within the MRF before decussating beneath the oculomotor nucleus (Grantyn and Grantyn, 1982; Moschovakis and Karabelas, 1985; Moschovakis et al., 1988a&b). Inputs from ipsilateral descending tectal pathways have been suggested in the goldfish (Luque et al., 2007), but this projection has not been reported in monkeys (Moschovakis et al., 1988a).

Thus, it seems likely that the MRF input labeled here is primarily from gaze-related neurons in the intermediate SC layers.

The distribution of reticulospinal neurons within the caudal MRF (i.e., the cMRF) has also been examined previously in primates (Castiglioni et al., 1978; Nudo and Masterton, 1988; Robinson et al., 1994; Warren et al., 2008). Similarly, the distribution patterns of reticulo- and interstitiospinal neurons shown here have been seen in the cat (Huerta and Harting, 1982; Zuk et al., 1983; Holstege, 1988; Spence and Saint-Cyr, 1988; Satoda et al., 2002) and the monkey (Castiglioni et al., 1978). Like previous primate studies (Castiglioni et al., 1978; Kokkoroyannis et al., 1996), we observed a predominantly ipsilateral distribution, but a more bilateral distribution was observed in cat studies (Edwards, 1975). A bilateral projection might be expected for vertical movements (Richmond et al., 1992; Corneil et al., 2001). However, these areas also subserve torsion (Crawford et al., 1991; Helmchen et al., 1996), and unilateral stimulation or loss of the InC and surrounding regions induces head tilt (Isa and Sasaki, 2002), which probably explains their predominantly unilateral projection.

Qualitative observations indicate that reticuloreticular neurons labeled in MRF following MdRF injections were more numerous than MRF reticulospinal cells (Compare Fig. 4 to Warren et al., 2008), and they generally displayed more close associations with tectoreticular terminals. This pattern of a meager direct projection to the cord, and a larger indirect projection via medullary reticulospinal neurons, parallels that seen in the tectospinal and tectoreticulospinal pathways (May and Porter, 1992), reinforcing the importance of the MdRF for organizing head turns.

The Trans-MRF Pathway

A striking finding from the present study is that the trans-MRF tectoreticulospinal pathway is predominantly ipsilateral (Fig. 13). Electrical stimulation of the SC produces a distinctive pattern of EMG activity in neck muscles used for head turns (Corneil et al., 2002a&b). Agonists for lateral head turns are activated, while the antagonists are inhibited, but sometimes display activity towards the end of the stimulation period. This suggests the direct, crossed tectoreticulospinal projection activates contralateral neck motoneurons that supply agonist muscles, while the most likely effect of the trans-MRF pathway is to inactivate neck motoneurons that supply ipsilateral antagonists (Richmond et al., 1992;Corneil et al., 2001). Since many MRF neurons continue firing after the gaze target is acquired (Waitzman et al., 1996) it is also possible that the trans-MRF pathway is responsible for the activity observed in EMGs of antagonists towards the end of SC stimulation, which may serve to brake the momentum of the head movement or stabilize the head at a new position (Roucoux et al., 1989).

A major contribution of this study is the demonstration that reticuloreticular neurons within the MRF are likely to receive input from the SC and project upon the MdRF (Fig. 13). The rostral MdRF is believed to play an important role in gaze-related head movements. Specifically, electrical stimulation of this region influences cervical motoneuron activity and produces head turns (Peterson et al., 1978;Drew and Rossignol, 1990a&b;Cowie and Robinson, 1994;Quessy and Freedman, 2004), while inactivation of this region affects head turns (Suzuki et al., 1989). Anatomical studies demonstrate that the MdRF reticulospinal population projects bilaterally (Mitani et al., 1988;Robinson et al., 1994). This bilateral pattern presumably represents connections underlying vertical head movements or that coordinate antagonist and agonist activity during horizontal head turns. While the medullary injections made here were not confined to MdRF regions implicated in head movement control, they certainly involved the medial rostral MdRF, where stimulation produces head movement. In addition, our recent anterograde studies indicate cMRF projections are confined to paramedian MdRF locations within the medulla (Zhou et al., 2006). Thus, it

appears that the trans-MRF pathway through the MdRF may act to support the role of the trans-MRF reticulospinal system, inhibiting antagonists and, in some cases activating muscles that are needed to stabilize cervical joints (Richmond et al., 1992;Thomson et al., 1996;Corneil et al., 2001), while those muscles activated by the direct tectoreticulospinal pathways produce the desired movement.

Feedback and Feed Forward Systems in the Macaque

The present results may speak to differences in the cMRF feedback and feed forward circuits. Observation of all our cases, revealed that labeled reticulotectal neurons clearly outnumbered labeled reticulomedullary neurons in the cMRF (Fig. 4& Fig. 7). This suggests that the feedback signal may be more central to cMRF function. In addition, previous studies (Chen and May, 2000;Warren et al., 2008) and examination of the present material indicated that the reticulotectal neurons consistently have more extensive tectoreticular terminal associations than reticuloreticular neurons. While some of this difference may be an artifact of the greater dendritic filling produced by BDA, it may also suggest that the feedback and descending pathway neurons in the MRF process SC input differently, and have different physiological signals. It is noteworthy then, that when Moschovakis and colleagues (1988b) investigated midbrain long lead burst neurons, only reticulotectal neurons were stained in the cMRF. It is also noteworthy that this head-related feed forward projection comes primarily from the medial MRF. Recently, we found evidence suggesting that the medial cMRF receives preferential input from tectospinal neurons (Zhou et al., 2008). Together these results indicate that there may be specialization with respect to function along the mediolateral axis of the MRF (Fig. 13). However, physiological studies only describe dorsoventral differences with respect to saccade amplitude (Cohen et al., 1985), and no obvious topography was observed for cells with head-related activity (Pathmanathan et al., 2006b). So these points require further examination in head-free preparations where feed forward and feedback units can be differentiated antidromically, in order to see how their signals and location differ.

Acknowledgments

The authors would like to express their gratitude to Olga Golanov, MD and Jennifer Cotton, RN for their assistance with the surgical procedures, histological work and help with illustrations. This work was done in partial fulfillment of a PhD degree by Eddie Perkins.

Grant Sponsor: National Institutes of Health; Grant # EY014263 (PJM & SW)

LITERATURE CITED

Anderson ME, Yoshida M, Wilson VJ. Influences of superior colliculus on cat neck motoneurons. J Neurophysiol. 1971; 34:898–907. [PubMed: 4328961]

André-Deshays C, Revel M, Berthoz A. Eye-head coupling in humans. II. Phasic components. Exp Brain Res. 1991; 84:359–366. [PubMed: 2065742]

Badler JB, Keller EL. Decoding of a motor command vector from distributed activity in superior colliculus. Biol Cybern. 2002; 86:179–189. [PubMed: 12068785]

Bender, MB.; Shanzer, S. Oculomotor pathways defined by electrical stimulation and lesion in the brainstem of the monkey. In: Bender, MB., editor. The Oculomotor System. New York: Harper and Row; 1964. p. 81-140.

Castiglioni AJ, Gallaway MC, Coulter JD. Spinal projections from the midbrain in monkey. J Comp Neurol. 1978; 178:329–346. [PubMed: 415074]

Chen B, May PJ. The feedback circuit connecting the superior colliculus and mesencephalic reticular formation: a direct morphological demonstration. Exp Brain Res. 2000; 131:10–21. [PubMed: 10759167]

Chen B, May PJ. Premotor control of eyelid movements in conjunction with vertical saccades in the cat: The rostral interstitial nucleus of the medial longitudinal fasciculus. J Comp Neurol. 2002; 450:183–202. [PubMed: 12124762]

Cohen, Büttner-Ennever JA. Projections from the superior colliculus to a region of the central mesencephalic reticular formation (cMRF) associated with horizontal saccadic eye movements. Exp Brain Res. 1984; 57:167–176. [PubMed: 6519224]

Cohen B, Matsuo V, Fradin J, Raphan T. Horizontal saccades induced by stimulation of the central mesencephalic reticular formation. Exp Brain Res. 1985; 57:605–616. [PubMed: 3979501]

Corneil BD, Olivier E, Richmond FJ, Loeb GE, Munoz DP. Neck muscles in the rhesus monkey. II. Electromyographic patterns of activation underlying postures and movements. J Neurophysiol. 2001; 86:1729–1749. [PubMed: 11600635]

Corneil BD, Olivier E, Munoz DP. Neck muscle responses to stimulation of monkey superior colliculus. I. Topography and manipulation of stimulation parameters. J Neurophysiol. 2002a; 88:1980–1999. [PubMed: 12364523]

Corneil BD, Olivier E, Munoz DP. Neck muscle responses to stimulation of monkey superior colliculus. II. Gaze shift initiation and volitional head movements. J Neurophysiol. 2002b; 88:2000–2018. [PubMed: 12364524]

Cowie RJ, Robinson DL. Subcortical contributions to head movements in macaques. I.Contrasting effects of electrical stimulation of a medial pontomedullary region and the superior colliculus. J Neurophysiol. 1994; 72:2648–2664. [PubMed: 7897481]

Cowie RJ, Smith MK, Robinson DL. Subcortical contributions to head movements in macaques. II. Connections of a medial pontomedullary head-movement region. J Neurophysiol. 1994; 72:2665–2682. [PubMed: 7534824]

Crawford JD, Cadera W, Vilis T. Generation of torsional and vertical eye position signals by the interstitial nucleus of Cajal. Science. 1991; 252:1551–1553. [PubMed: 2047862]

Cromer JA, Waitzman DM. Neurons associated with saccade metrics in the monkey central mesencephalic reticular formation. J Physiol. 2006; 570:507–523. [PubMed: 16308353]

Cromer JA, Waitzman DM. Comparison of saccade-associated neuronal activity in the primate central mesencephalic and paramedian pontine reticular formations. J Neurophysiol. 2007; 98:835–850. [PubMed: 17537904]

Drew T, Rossignol S. Functional organization within the medullary reticular formation of intact unanesthetized cat. I. Movement evoked by microstimulation. J Neurophysiol. 1990a; 64:767–781. [PubMed: 2230923]

Drew T, Rossignol S. Functional organization within the medullary reticular formation of intact unanesthetized cat. II. Electromyographic activity evoked by microstimulation. J Neurophysiol. 1990b; 64:782–795. [PubMed: 2230924]

Dunham DN. Cognitive difficulty of a peripherally presented visual task affects head movements during gaze displacement. Int J Psychophysiol. 1997; 27:171–112. [PubMed: 9451577]

Edwards SB. Autoradiographic studies of the projections of the midbrain reticular formation: descending projections of nucleus cuneiformis. J Comp Neurol. 1975; 161:341–538. [PubMed: 50329]

Freedman EG, Sparks DL. Activity of cells in the deeper layers of the superior colliculus of the rhesus monkey: Evidence for a gaze displacement command. J Neurophysiol. 1997a; 78:1669–1690. [PubMed: 9310452]

Freedman EG, Sparks DL. Eye-head coordination during head-unrestrained gaze shifts in rhesus monkeys. J Neurophysiol. 1997b; 77:2328–2348. [PubMed: 9163361]

Freedman EG, Sparks DL. Coordination of the eyes and head: movement kinematics. Exp Brain Res. 2000; 131:22–32. [PubMed: 10759168]

Fukushima K, Hirai N, Rapoport S. Direct excitation of neck flexor motoneurons by the interstitiospinal tract. Brain Res. 1979; 160:358–362. [PubMed: 761070]

Fukushima K, Ohashi T, Fukushima J, Kaneko CRS. Discharge characteristics of vestibular and saccade neurons in the rostral midbrain of alert cats. J Neurophysiol. 1995; 73:2129–2143. [PubMed: 7666128]

Fuller JH. Head movement propensity. Exp Brain Res. 1992; 92:152–164. [PubMed: 1486950]

Grantyn A, Grantyn R. Axonal patterns and sites of termination of cat superior colliculus neurons projecting in the tecto-bulbo-spinal tract. Exp Brain Res. 1982; 46:243–256. [PubMed: 7095033]

Guitton D, Douglas RM, Volle M. Coordinated eye-head movements in the cat. J.Neurophysiol. 1984; 52:1030–1050. [PubMed: 6335170]

Handel A, Glimcher PW. Response properties of saccade-related burst neurons in the central mesencephalic reticular formation. J Neurophysiol. 1997; 78:2164–2175. [PubMed: 9325383]

Harting JK. Descending pathways from the superior colliculus: An autoradiographic analysis in the rhesus monkey (*Macaca mulatta*). J Comp Neurol. 1977; 173:583–612. [PubMed: 404340]

Helmchen C, Rambold H, Büttner U. Saccade-related burst neurons with torsional and vertical on directions in the interstitial nucleus of Cajal of the alert monkey. Exp Brain Res. 1996; 112:63–78. [PubMed: 8951408]

Holstege, G. Brainstem-spinal cord projections in the cat, related to control of head and axial movements. In: Büttner-Ennever, JA., editor. Neuroanatomy of The Oculomotor System. New York: Elsevier Press; 1988. p. 431-470.

Huerta MF, Harting JK. Tectal control of spinal cord activity: neuroanatomical demonstration of pathways connecting the superior colliculus with the cervical spinal cord grey. Prog Brain Res. 1982; 57:293–328. [PubMed: 6296921]

Isa T, Sasaki S. Brainstem control of head movements during orienting: organization of the premotor circuits. Prog Neurobiol. 2002; 66:205–241. [PubMed: 11960679]

Iwamoto Y, Sasaki S, Susuki I. Descending cortical and tectal control of dorsal neck motoneurons via reticulospinal neurons in the cat. Prog Brain Res. 1988; 76:97–108. [PubMed: 3064162]

Kakei S, Muto N, Shinoda Y. Innervation of multiple neck motor nuclei by single reticulospinal tract axons receiving tectal input in the upper cervical spinal cord. Neurosci Let. 1994; 172:85–88. [PubMed: 8084543]

King WM, Precht W, Dieringer N. Synaptic organization of frontal eye field and vestibular afferents to interstitial nucleus of Cajal in the cat. J Neurophysiol. 1980; 43:912–908. [PubMed: 7359181]

Kokkoroyannis T, Schudder CA, Balaban CD, Highstein SM, Moschovakis AK. Anatomy and physiology of the primate interstitial nucleus of Cajal. I. Efferent projections. J Neurophysiol. 1996; 75:725–739. [PubMed: 8714648]

Luque MA, Perez-Perez MP, Herrero L, Torres B. Connections of eye-saccade-related areas within mesencephalic reticular formation with optic tectum in goldfish. J Comp Neurol. 2007; 500:6–19. [PubMed: 17099899]

May PJ. The mammalian superior colliculus: laminar structure and connections. Prog Brain Res. 2006; 151:321–378. [PubMed: 16221594]

May, PJ.; Warren, S.; Chen, B.; Richmond, FJR.; Olivier, E. Midbrain reticular formation circuitry subserving gaze in the cat. In: Kaminsky, HJ.; Leigh, RJ., editors. Neurobiology of Eye Movements from Molecules to Behavior. An NY Acad Sci. Vol. 956. 2002. p. 405-408.

May PJ, Perkins E, Zhou L, Warren S. Macaque central mesencephalic reticular formation connections underlying collicular control of gaze. Soc Neurosci Abst. 2005; 31:858.4.

May PJ, Porter JD. The laminar distribution of macaque tectobulbar and tectospinal neurons. Visual Neurosci. 1992; 8:257–276.

Mitani A, Ito K, Mitani Y, McCarley RW. Descending projections from the gigantocellular tegmental field in the cat: cells of origin and their brainstem and spinal cord trajectories. J Comp Neurol. 1988; 268:546–566. [PubMed: 2451685]

Moschovakis AK, Karabelas AB. Observations on the somatodendritic morphology and axonal trajectory of intracellularly HRP-labeled efferent neurons located in the deeper layers of the superior colliculus of the cat. J Comp Neurol. 1985; 239:276–308. [PubMed: 4044941]

Moschovakis AK, Karabelas AB, Highstein SM. Structure-function relationships in the primate superior colliculus. I. Morphological classification of efferent neurons. J Neurophysiol. 1988a; 60:232–262. [PubMed: 3404219]

Moschovakis AK, Karabelas AB, Highstein SM. Structure-function relationships in the primate superior colliculus. II. Morphological identity of presaccadic neurons. J Neurophysiol. 1988b; 60:263–302. [PubMed: 3404220]

Moschovakis AK, Kitama T, Dalezios Y, Petit J, Brandi AM, Grantyn AA. An anatomical substrate for the spatiotemporal transformation. J Neurosci. 1998; 18:10219–10229. [PubMed: 9822775]

Mustari MJ, Fuchs AF, Kaneko CR, Robinson FR. Anatomical connections of the primate pretectal nucleus of the optic tract. J Comp Neurol. 1994; 349:111–128. [PubMed: 7852621]

Nudo RJ, Masterton RB. Descending pathways to the spinal cord: II. Quantitative study of the tectospinal tract in 23 mammals. J Comp Neurol. 1989; 286:96–119. [PubMed: 2768559]

Pathmanathan JS, Presnell R, Cromer JA, Cullen KE, Waitzman DM. Spatial characteristics of neurons in the central mesencephalic reticular formation (cMRF) of head-unrestrained monkeys. Exp Brain Res. 2006a; 168:455–470. [PubMed: 16292575]

Pathmanathan JS, Cromer JA, Cullen KE, Waitzman DM. Temporal characteristics of neurons in the central mesencephalic reticular formation of head unrestrained monkeys. Exp Brain Res. 2006b; 168:471–492. [PubMed: 16292574]

Peterson BW, Pitts NG, Fukushima K, Mackel R. Reticulospinal excitation and inhibition of neck motoneurons. Exp Brain Res. 1978; 32:471–489. [PubMed: 689126]

Quessy S, Freedman EG. Electrical stimulation of rhesus monkey nucleus reticularis gigantocellularis. I. Characteristics of evoked head movements. Exp Brain Res. 2004; 156:342–356. [PubMed: 14985893]

Richmond, FJR.; Gordon, E.; Loeb, GE. Heterogeneous structure and function among intervertebral muscles. In: Berthoz, A.; Vidal, PP.; Graf, W., editors. The Head-Neck Sensory Motor System. Oxford: Oxford University Press; 1992. p. 141-147.

Robinson FR, Phillips JO, Fuchs AF. Coordination of gaze shifts in primates: brainstem inputs to neck and extraocular motoneurons pools. J Comp Neurol. 1994; 346:43–62. [PubMed: 7962711]

Ron S, Berthoz A. Eye and head coupled and dissociated movements during orientation to a double step visual target displacement. Exp Brain Res. 1991; 85:196–207. [PubMed: 1884758]

Rose PK, MacDonald J, Abrahams VC. Projections of the tectospinal tract to the upper cervical spinal cord of the cat: A study with the anterograde tracer PHA-L. J Comp Neurol. 1991; 314:91–105. [PubMed: 1797878]

Roucoux A, Guitton D, Crommelinck M. Stimulation of the superior colliculus in the alert cat. II. Eye and head movements evoked when the head is unrestrained. Exp Brain Res. 1980; 39:75–85. [PubMed: 7379887]

Roucoux A, Crommelinck M, Decostre MF. Neck muscle activity in eye-head coordinated movements. Prog Brain Res. 1989; 80:351–362. [PubMed: 2634276]

Satoda T, Matsumoto H, Zhou L, Rose PK, Richmond FJR. Mesencephalic projections to the first cervical segment in the cat. Exp Brain Res. 2002; 144:397–413. [PubMed: 12021821]

Scudder CA, Moschovakis AK, Karabelas AB, Highstein SM. Anatomy and physiology of saccadic long-lead burst neurons recorded in the alert squirrel monkey. I. Descending projections from the mesencephalon. J Neurophysiol. 1996a; 76:332–352. [PubMed: 8836229]

Scudder CA, Moschovakis AK, Karabelas AB, Highstein SM. Anatomy and physiology of saccadic long-lead burst neurons recorded in the alert squirrel monkey. II. Pontine neurons. J Neurophysiol. 1996b; 76:353–370. [PubMed: 8836230]

Sparks DL. Translation of sensory signals into commands for control of saccadic eye movements: role of primate superior colliculus. Physiol Rev. 1986; 66:118–171. [PubMed: 3511480]

Spence SJ, Saint-Cyr JA. Comparative topography of projections from the mesodiencephalic junction to the inferior olive, vestibular nuclei, and upper cervical cord in cats. J Comp Neurol. 1988; 268:357–374. [PubMed: 3360994]

Stahl JS. Amplitude of human head movements associated with horizontal saccades. Exp Brain Res. 1999; 126:41–54. [PubMed: 10333006]

Stahl JS. Adaptive plasticity of head movement propensity. Exp Brain Res. 2001; 139:201–208. [PubMed: 11497062]

Stryker MP, Schiller PH. Eye and head movements evoked by electrical stimulation of monkey superior colliculus. Exp Brain Res. 1975; 23:103–112. [PubMed: 1149845]

Suzuki SS, Siegel JM, Wu MF. Role of pontomedullary reticular neurons in horizontal head movements: an ibotenic acid lesion study in the cat. Brain Res. 1989; 484:78–93. [PubMed: 2713704]

Sylvestre PA, Cullen KE. Premotor correlates of integrated feedback control for eye-head gaze shifts. J Neurosci. 2006; 26:4922–4929. [PubMed: 16672667]

Szabo J, Cowan WM. A Stereotaxic Atlas of the brain of the cynomolgus monkey (*Macaca fascicularis*). J Comp Neurol. 1984; 222:265–300. [PubMed: 6365984]

Thomson DB, Loeb GE, Richmond FJR. Effect of neck posture on patterns of activation of feline neck muscles during horizontal rotation. Exp Brain Res. 1996; 110:392–400. [PubMed: 8871098]

Tweed D, Glenn B, Vilis T. Eye-head coordination during large gaze shifts. J Neurophysiol. 1995; 73:766–779. [PubMed: 7760133]

Waitzman DM, Silakov VL, Cohen B. Central mesencephalic reticular formation (cMRF) neurons discharging before and during eye movements. J Neurophysiol. 1996; 75:1546–1572. [PubMed: 8727396]

Waitzman DM, Silakov VL, DePalma-Bowles S, Ayers AS. Effects of reversible inactivation of the primate mesencephalic reticular formation. II. Hypometric vertical saccades. J Neurophysiol. 2000a; 83:2285–2299. [PubMed: 10758134]

Waitzman DM, Silakov VL, DePalma-Bowles S, Ayers AS. Effects of reversible inactivation of the primate mesencephalic reticular formation. I. Hypermetric goal-directed saccades. J Neurophysiol. 2000b; 83:2260–2284. [PubMed: 10758133]

Walton MMG, Bechara B, Gandhi NJ. Role of primate superior colliculus in the control of head movements. J Neurophys. 2007; 98:2022–2037.

Warren S, Waitzman DM, May PJ. Anatomical evidence for interconnections between the central mesencephalic reticular formation and cervical spinal cord in the cat and macaque. Anat Rec. 2008; 291:141–160.

Zhou L, Warren S, May PJ. Projection of the central mesencephalic reticular formation in the macaque. Soc Neurosci Abst. 2006; 32:139.1.

Zhou L, Warren S, May PJ. The feedback circuit connecting the central mesencephalic reticular formation and the superior colliculus in the macaque monkey: Tectal connections. Exp. Brain Res. 2008; 189:485–496. [PubMed: 18553075]

Zuk A, Rutherford JG, Gwyn DG. Projections from the interstitial nucleus of Cajal to the inferior olive and to the spinal cord in cat: a retrograde fluorescent double-labeling study. Neurosci Lett. 1983; 38:95–101. [PubMed: 6312383]

ABBREVIATIONS

III	oculomotor nucleus
IV	trochlear nucleus
VI	abducens nucleus
VII	facial nucleus
VIIn	facial nerve
XII	hypoglossal nucleus
BDA	biotinlyated dextran amine
BC	brachium conjuntivum
C	cuneate nucleus
C1-3	cervical cord levels 1–2
CC	caudal central subdivision of III
cMRF	central mesencephalic reticular formation
DR	dorsal raphe
EW_{pg}	Edinger-Westhpal nucleus, preganglionic

G	gracile nucleus
IC	inferior colliculus
InC	interstitial nucleus of Cajal
IO	inferior olive
MdRF	medullary reticular formation
MLF	medial longitudinal fasciculus
nD	nucleus of Darkschiewitsch
nOT	nucleus of the optic tract
nPC	nucleus of the posterior commissure
P	pyramid
PAG	periaqueductal gray
PB	parabrachial nuclei
PC	posterior commissure
PhaL	*Phaseolus vulgaris* leukoagglutinin
PRF	pontine reticular formation
PPRF	paramedian pontine reticular formation
piMRF	peri-InC mesencephalic reticular formation
Pt	pretectum
Pul	pulvinar
PVG	periventricular gray
R	red nucleus
SC	superior colliculus
SGI	intermediate gray layer of superior colliculus
SGS	superficial gray layer of superior colliculus
SN	substantia nigra
SO	superior olive
SOA	supraoculomotor area
VH	ventral horn
VN	vestibular nuclei
Vs	trigeminal sensory nucleus
WGA-HRP	wheat germ agglutinin conjugated horseradish peroxidase

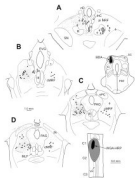

Figure 1.
Pattern of labeling in the MRF following a BDA injection in the left superior colliculus (SC) (charting, upper right) and WGA-HRP injection in the left upper cervical spinal cord (charting, lower right). A–D show the locations of BDA labeled tectoreticular terminals (stipple), and BDA labeled reticulotectal neurons (dots), as well as WGA-HRP labeled reticulospinal neurons (diamonds) in an rostrocaudal series of individual sections. Note the medial location of the reticulospinal neurons. Each dot and diamond represents a single neuron in individual sections lying approximately 600 μm apart in this and other chartings. In this and other illustrations, the core of the injections site is drawn as black, and the outer limits of the tracer spread are indicated as gray.

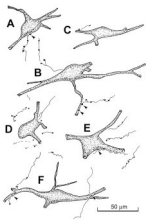

Figure 2.
Examples of WGA-HRP labeled neurons and BDA labeled axons in the MRF from the case shown in figure 1. Close associations between the boutons of BDA labeled tectoreticular axons and cells in piMRF (A&B) and cMRF (C–F) are indicated by arrowheads.

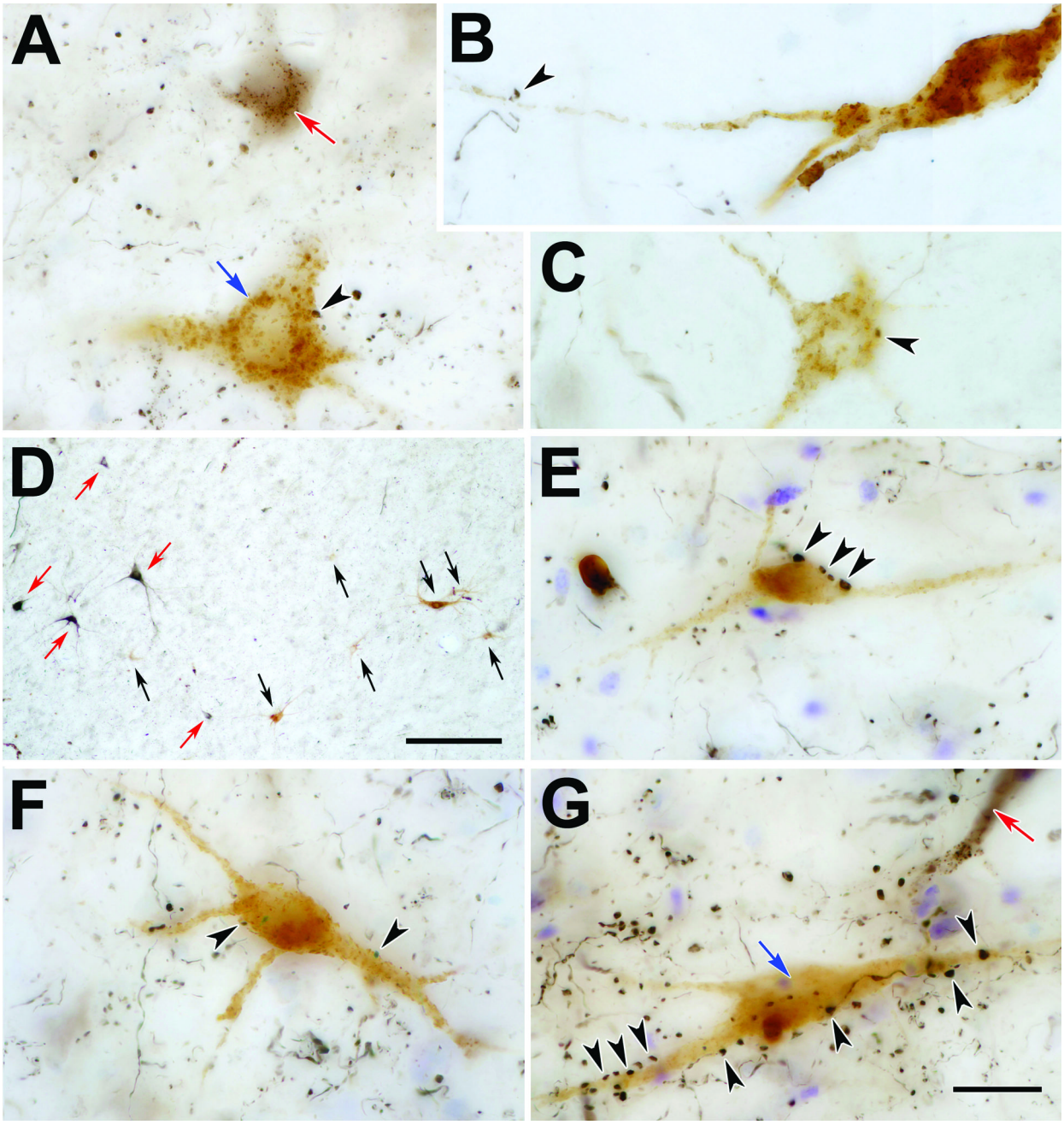

Figure 3.

Photomicrographs showing associations between WGA-HRP labeled neurons and BDA labeled tectoreticular terminals within the piMRF (C, E) and cMRF (A,B,D,F&G). Panels A–C show tectospinal neurons from cases like that illustrated in figure 1&figure 2. In A, a brownish-black BDA labeled tectoreticular neuron (red arrow) and a golden-brown WGA-HRP labeled reticulospinal neuron may be compared. A–C show examples of close associations (arrowheads) between the somata (A&C) and dendrites (B) of WGA-HRP labeled neurons and BDA labeled tectoreticular boutons (arrow heads). Panels E–G show examples of reticuloreticular neurons labeled following WGA-HRP injections in MdRF. The difference in color and location between the brownish-black, BDA labeled, reticulotectal neurons (red arrows) and the golden-brown, WGA-HRP labeled, reticuloreticular neurons

(black arrows) is evident in D. Close associations (arrowheads) are evident between the boutons of black, BDA labeled tectoreticular axons and examples of WGA-HRP labeled reticuloreticular neurons (E–G). Scale bar in D = 0.25 mm. in G = 20 μm Scale in G = A–C,E&F. Z axis planes for A&G=16, B&C=8, D=10, E&F=20.

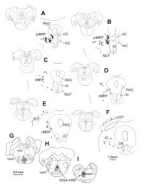

Figure 4.
Distribution of retrogradely labeled reticuloreticular cells (dots) within the MRF (A–F) following an injection of WGA-HRP into the MdRF (G–I).

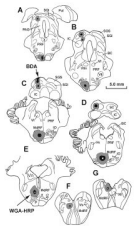

Figure 5.
Chartings of the injections sites for BDA in the superior colliculus (A–D) and for WGA-HRP in the medullary reticular formation (D–F) for the case illustrated in figure 6–figure 8.

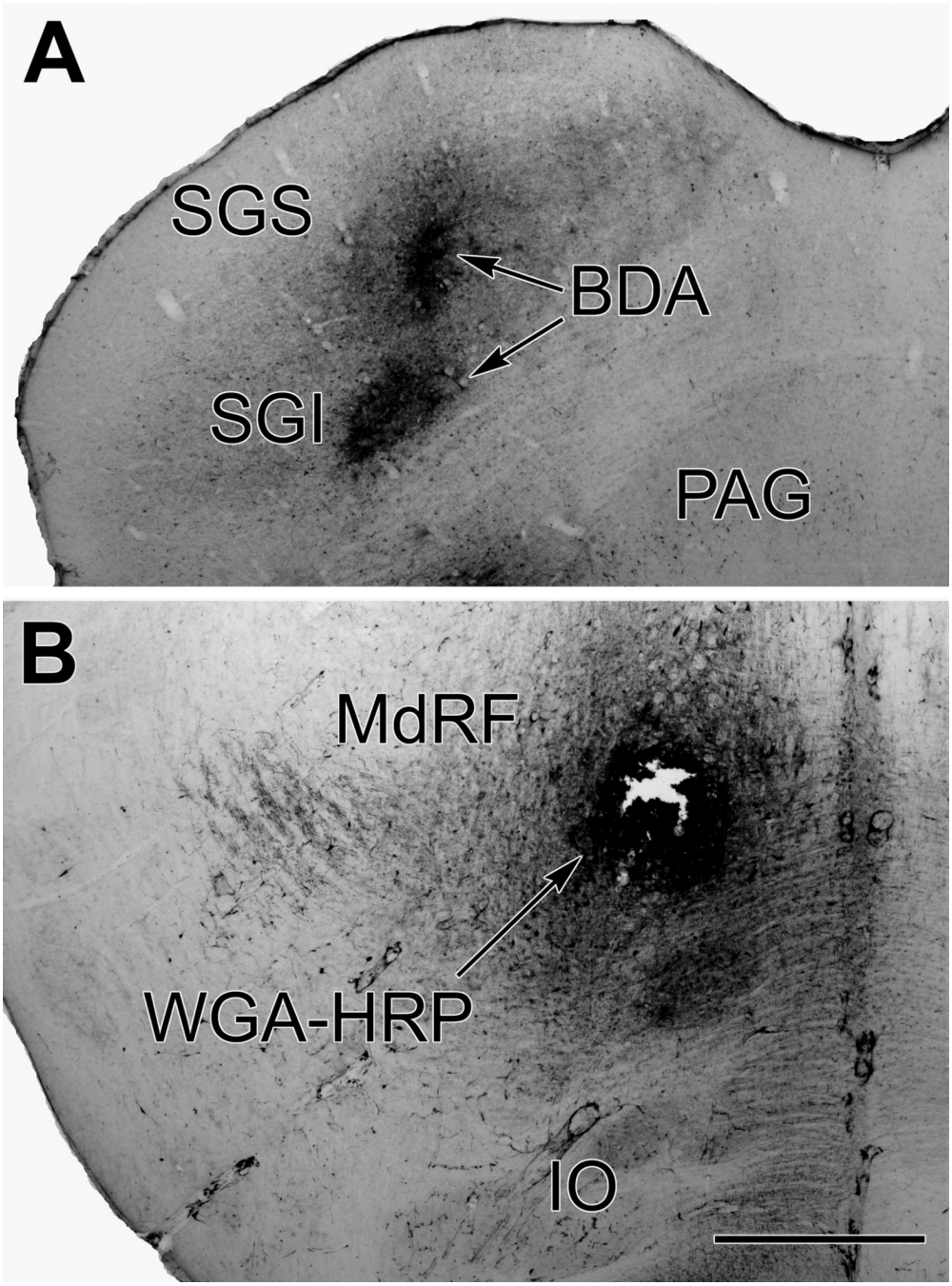

Figure 6.
Photomicrographs showing the appearance of the BDA injection site in the superior colliculus (A) and the WGA-HRP injection site in the medullary reticular formation (B) from the case illustrated in figure 5. Scale bar = 1.0 mm.

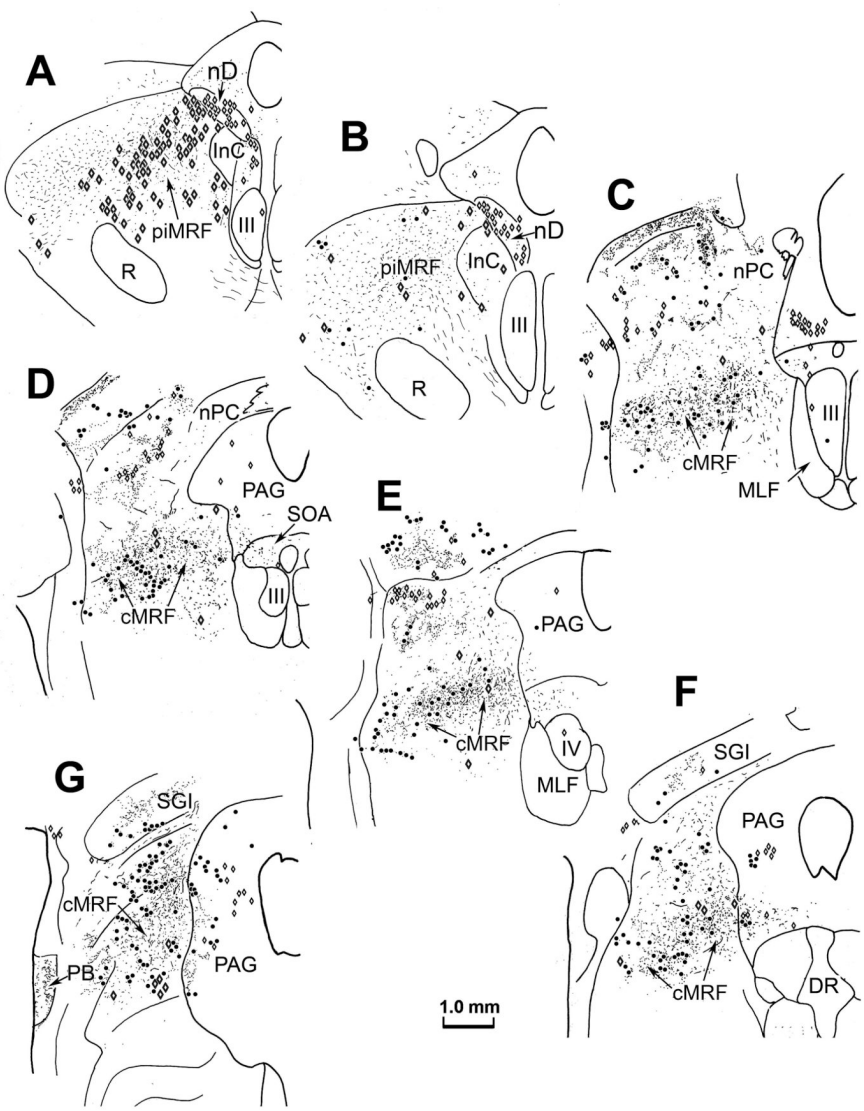

Figure 7.

Distribution of tectoreticular terminals, reticulotectal neurons and reticuloreticular neurons within the ipsilateral MRF following the injections illustrated in figure 5. Note the overlapping distributions of BDA labeled tectoreticular terminals (stipple), BDA labeled reticulotectal cells (black dots) and WGA-HRP labeled reticuloreticular cells (diamonds) within the piMRF (A&B) and cMRF (C–G).

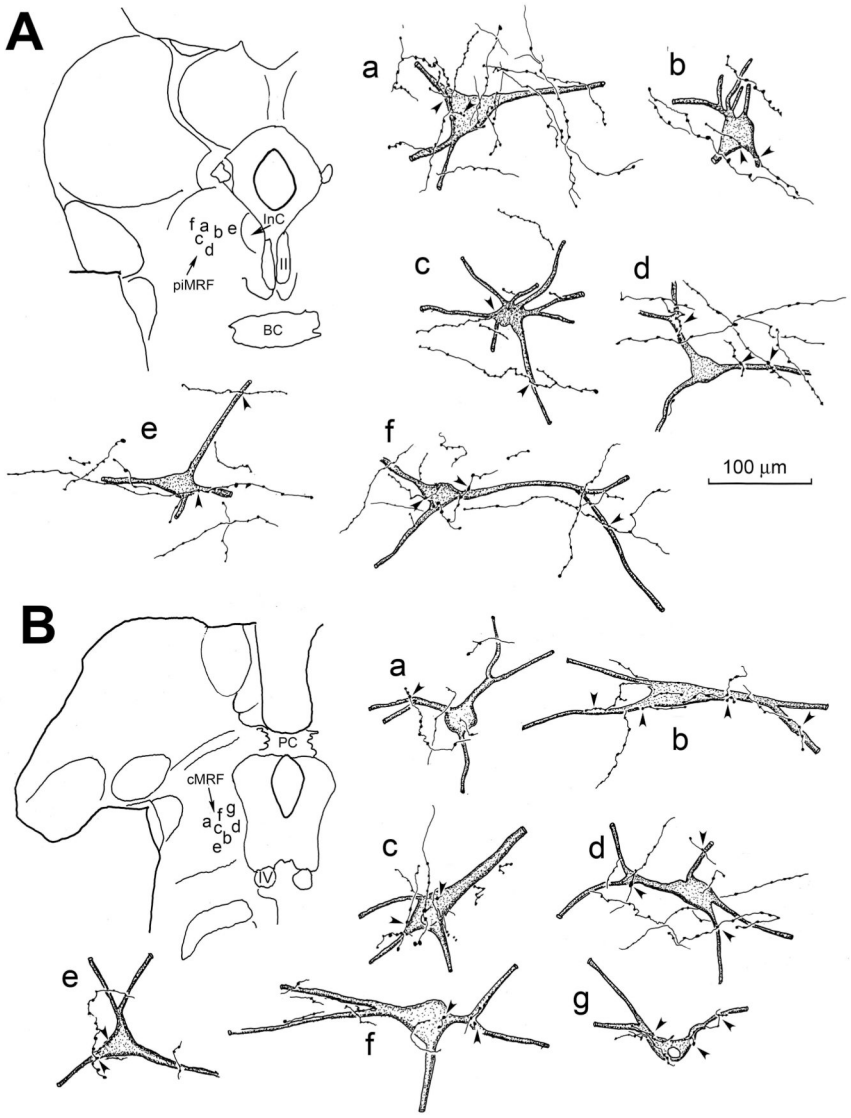

Figure 8.

Relationship between BDA labeled tectoreticular inputs and WGA-HRP labeled reticuloreticular neurons in the piMRF (A) and cMRF (B). In both cases, close associations, suggestive of synaptic contact, between the BDA labeled tectoreticular terminals and WGA-HRP labeled reticuloreticular neurons were observed (arrowheads). Inserts on the left indicate the locations of the illustrated cells.

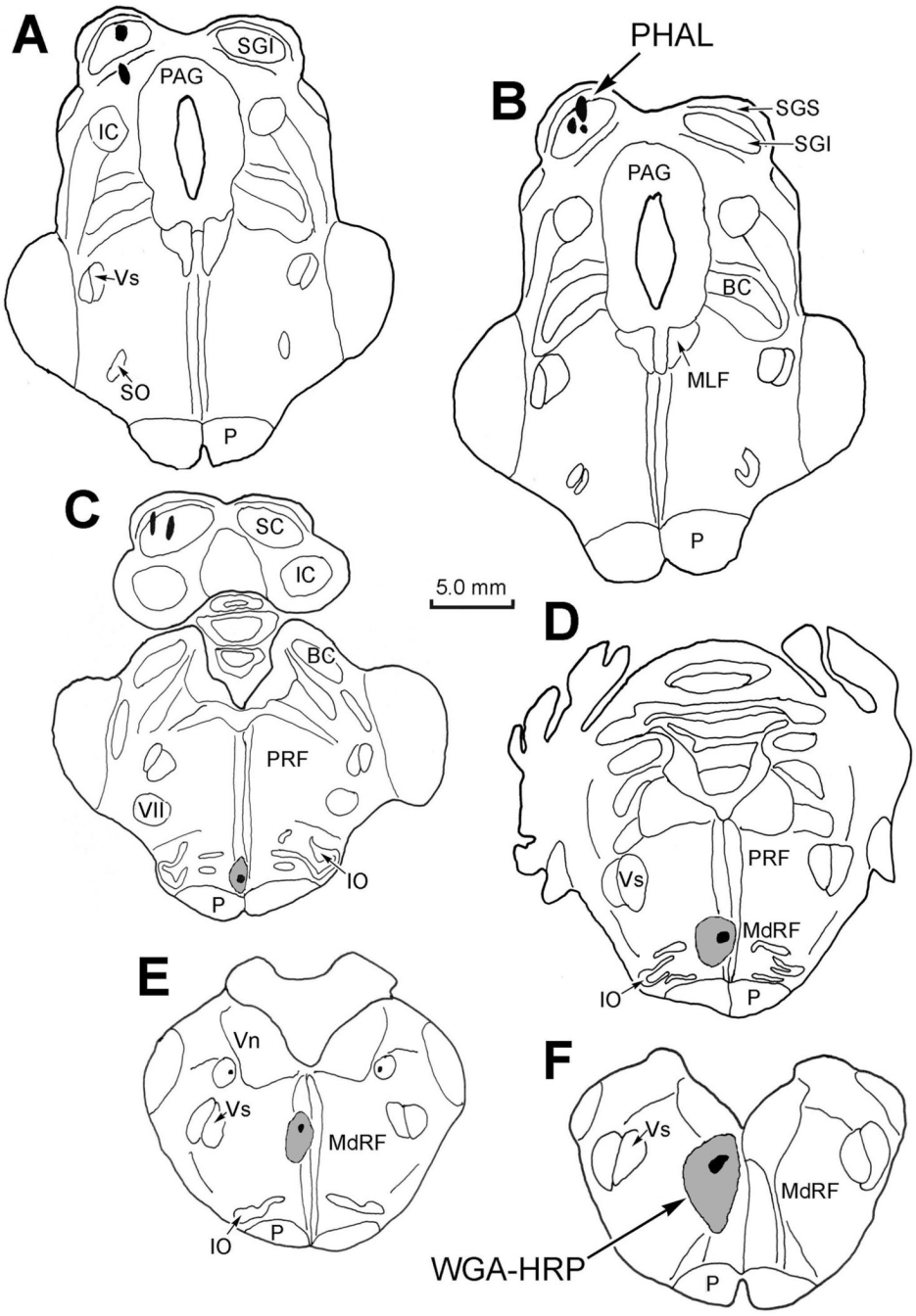

Figure 9.
Extent of a PhaL injection in the left superior colliculus (A–C) and WGA-HRP injection into the left medullary reticular formation (C–E) for the case illustrated in figure 10&figure 11.

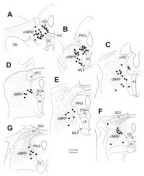

Figure 10.
Distribution of tectoreticular terminals and reticuloreticular neurons within the MRF. The overlapping distribution of PhaL labeled tectoreticular terminals (stipple) and WGA-HRP labeled reticuloreticular cells (dots) is illustrated in sections through the piMRF (A&B) and cMRF (C–G).

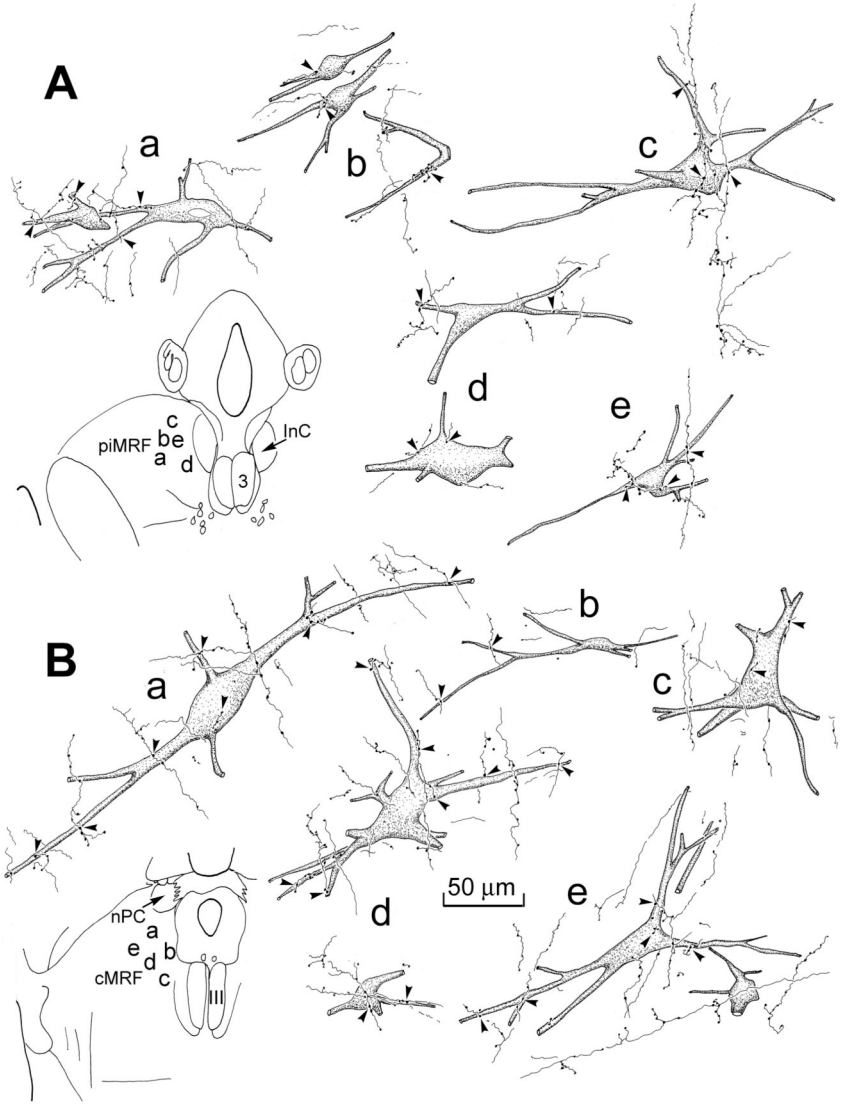

Figure 11.
Examples of tectoreticular terminals and reticuloreticular neurons in the piMRF (A) and cMRF (B). The PhaL labeled tectoreticular terminals display boutons which have close associations (arrowheads) with both the somata and dendrites of WGA-HRP labeled reticuloreticular neurons. Location of examples shown in inserts on left.

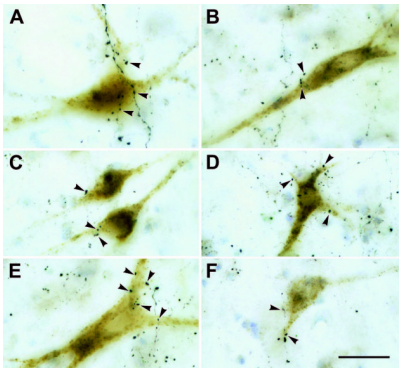

Figure 12.
Photomicrographs showing reticuloreticular neurons labeled following medullary injections of WGA-HRP and tectoreticular axons labeled with PhaL in the piMRF (A&B) and cMRF (C–F). The boutons of the PhaL labeled axons often lie in close association (arrowheads) with the retrogradely labeled reticuloreticular neurons. Scale bar = 30 μm. Z axis planes for A=11, B=7, C=11, D=19, E=10, F=9.

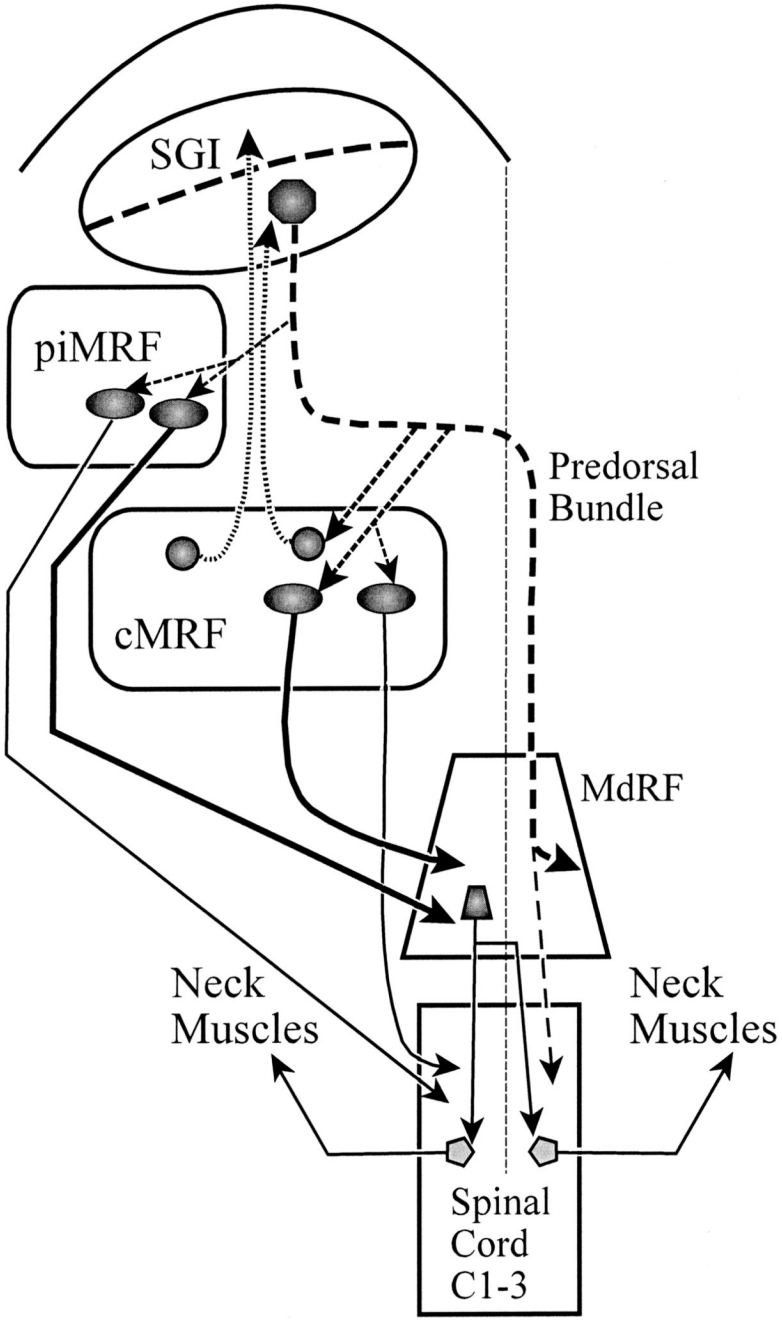

Figure 13.

Circuit diagram showing the direct and trans-MRF pathways by which the SC gains access to brainstem and spinal cord centers controlling head movements during a gaze change. The circuit diagram shows the decussating predorsal bundle pathway (dashed line) in the context of the MRF projections. Neurons in the medial part of the piMRF and cMRF provide a site for the SC to directly modulate spinal cord activity (thin line) and indirectly control the activity of cervical motoneurons via the MdRF (thick line). The cMRF also provides feedback to the SC (dotted line).